Journal of
NUCLEAR
Technology in Applied Science
ISSN 2314-8209 e-ISSN 2314-8217

J. Nucl. Tech. Appl. Sci, Vol. 5, No. 4, PP. 183 : 203 (2017)

Numerical Simulation of Groundwater Flow and Solute Transport in Shallow Aquifer of Wadi El-Natrun West Delta Egypt

Gad, M.I.[1]; Hussien, R.A.[2*] and El- Aassar, A.M.[3]

Received: 27/08/2017
Accepted: 08/10/2017

E.mail:Rasha.enrra@gmail.com

ABSTRACT

To face the sharp increase of population in Egypt, new areas are being reclaimed. In the new reclaimed areas in Wadi El-Natrun, the groundwater is considered the main water resource for the irrigation purposes. In order to optimize and conserve the use of groundwater in these areas, some strategies should be considered, such as managing the supply and the demand, improving the efficiency of groundwater use, reducing the heavy metals transport and ensuring sustainability. For predicting the change in the groundwater system of the study area as a result of random reclamation projects, a quasi-three dimensional groundwater flow model (Visual MODFLOW) for planning and managing the groundwater problems was applied in this paper. Chemical results clarified that the presence of two: northwestern (slightly saline) and southeastern zones (moderately saline) that varied in their hydro-chemical characteristics. Trace elements concentration for Al, Fe and Sr are exceeding the acceptable limits in compared to WHO (2011). The simulation results show that the recharge to shallow aquifer from the flash flood event at 2015 increases the piezometric head from 0.23m to 0.64m with a mean value of 0.45m. Otherwise, the predicted piezometric head contour map applying 2nd scenario reflects the disappearance of the cone of depression related to 1st scenario which reappears again after 50 years. On the other side, the results of the fourth scenario which deals with the simulation of the heavy metal contaminant transport shows that the plume of the three con-

KEYWORDS

Hydrochemistry, Heavy Metals, MODFLOW, Contaminant Transport Simulation, Wadi El-Natrun.

1. Hydrology Dept. Desert Research Center, Cairo, Egypt
2. Siting and Environment Depart. Egyptian Nuclear and Radiological Regulatory Authority (ENRRA)
3. Hydrogeochemistry Department, Desert Research Center, Cairo, Egypt.
*Corresponding author

taminants (Al, Fe and Sr) is different in shape and direction. They travel 10.1, 11 and 12 km due west direction and 13.5, 9 and 10.2 km due SW direction after 50 years of simulation. Based on these results, it is highly recommended to apply discrete irrigation system and achieving the objective of implementing the development policy with the groundwater recharge from the flash flood events. It is also recommended to construct a monitoring network to check the predicted contaminant plume migration distance to test the uncertainty of the model results.

INTRODUCTION

In arid and semi-arid regions, domestic, industrial and agricultural water uses depend mainly on groundwater resources. However, due to unsuitable management of water resources, several problems related to groundwater use have arisen, such as the extraordinary decline of the groundwater level coupled with salinization and resource pollution ***(*Liu *et al., 2001;* Dassi *et al., 2005;* Fehdi *et al., 2009)***. Dynamics and hydrochemistry of the groundwater under a range of management practices for a given combination of climate, land cover, soil, and irrigation is necessary to devise practices to conserve and effectively use the water resources, without adverse impacts on groundwater quality and quantity **(Foster and Chilton, 2003; Jianhua *et al*., 2008; Edmunds, 2009; Dassi, 2010; Zagonari, 2010).** Sustainable control of water resources with sufficient understanding of the groundwater situation is therefore essential. An example of ever-deterioration in the conditions of the groundwater resources is striking in Wadi El-Natrun area in Egypt. The Egyptian government has undertaken a program for exploiting the Pliocene aquifer of Wadi El-Natrun area since 1962 to support reclamation practices and to settle new communities out of the Nile valley and the Delta regions. As a result, 45 production wells were drilled in and around Wadi El-Natrun under the supervision of the General Desert Development Organization (GDDO). Most of these wells are distributed parallel to Cairo-Alexandria Desert road **(Fig.1)**. In 1962, water extraction from the aquifer started with about 4 X 10^6 m^3/year and increased up to 72 X 10^6 m^3/year in 1999 **(RIGW, 2004).** Of this extraction, more than 90% has been used to sustain extensive agricultural needs of water. Recharge rates, however, have not kept pace with extraction and have generally been less than the total discharge of the aquifer (i.e., extraction, evapo-transpiration and losses to lakes). These have led to degradation of the groundwater conditions, both quantity and quality. Documenting changes in the spatio-temporal conditions of the groundwater and highlighting environmental factors that may have a great bearing on the area's groundwater aquifers extent and the geochemical variations of the available water types became a must. This could help prioritizing areas where efforts and sustainable development based on proper management plans should be focused.

Site Description and climate

Wadi El-Natrun is an elongated depression attaining a length of about 50 km and a width ranging from 5 to 10 km. It is located between latitudes 30° 15' and 30° 33'N, and longitudes 30° 00' and 30°33'E. It covers an area of about 500 km^2 (Fig. 1). The lowest point of the depression is about 23 m below sea level, whereas the general lowland area of the depression is about 50 m below the level of its borders. A series of ten large, elongated salt water lakes occupy the central lower part of the depression. They extend from the southeast to the northwest direction. Its climate is characterized by a long hot summer and a short warm winter; the maximum air temperature is reached in August and lies typically at about 36 ^{0}C, whereas the minimum air temperature of about 6ºC is observed in February. The mean annual rainfall reaches 30 mm/y and the relative humidity is generally higher in the summer season than

in winter. The annual relative humidity ranges from 69.2 % at El Tahrir district and 53.7 % at Wadi El Natrun. The area also characterized by a high evaporation rate, e.g. about 13.8 mm/day in June..

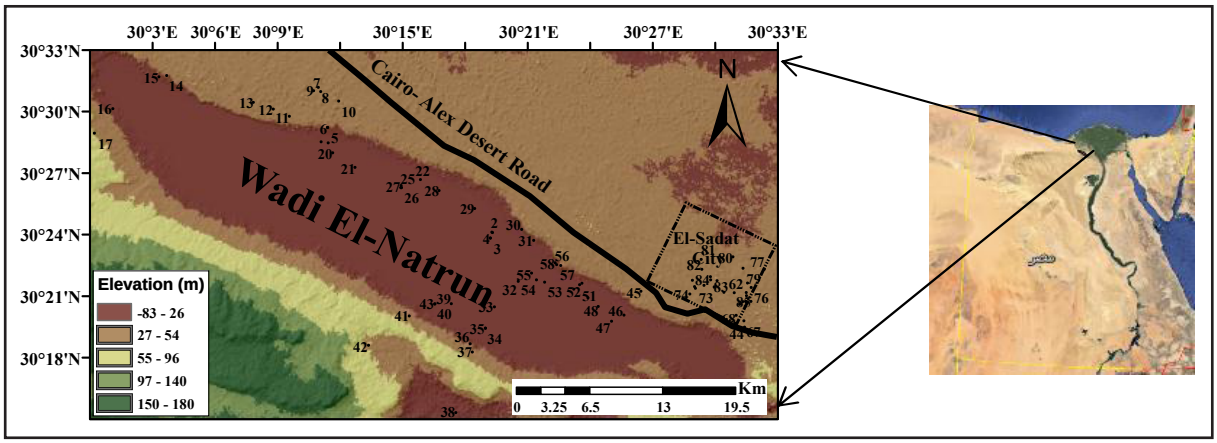

Fig. (1): Location map of the study area and Topography (m) with collected water samples.

Geomorphological and geological setting

The geomorphology of the study area is studied early by different authors. The landforms of the area reflect the effect of both geologic structure and the prevailed climatic conditions during their formations. Geomorphologically, the area of Wadi El Naturn is characterized by the old alluvial plains, the structural plains and the tablelands. The old alluvial plains, occupying the generally flat area between Rosetta branch to Wadi El Natrun and extends northward to Maryut tableland. It is a rolling plain sloping to the north and northeast and covered with sand sheets. The structural plains occupy a wide area to the south and west of the old alluvial plains. It consists of a number of alternating ridges and depressions, reflecting the impact of both lithological and geological structure. The structural ridges include Dahr El Tashasha – Khashm El Kaoud ridge (110 to 150 m a.m.s.l height) and El Washika – El Qantara synclinal ridge (180 to 190 m a.m.s.l height), while the structural depressions include Wadi El- Natrun depression (23 m u.m.s.l) Wadi El-Farigh depression (4 m u.m.s.l) and Wadi El-Tarfaya depression. The tablelands include, El-Alam tableland (120 m a.m.s.l) and Gebel El-Hadid tableland (160 m a.m.s.l).

Geologically, the area under consideration is occupied by sedimentary rocks ranging in age from Miocene to Quaternary time. According to **Said (1962); El Fayoumi (1964)** and **Omara and Sanad (1975)** the subsurface sequence belongs to the Pre-Miocene rocks with 3500m thickness till the basement. The upper part of this sequence is dominated by sand and clay facies while the lower part is characterized by lime and shale facies. Structurally, the detected folds in the study area are Wadi El-Natrun anticline (N35° W direction and 60 km extension) and Wadi El-Farigh anticline (NW-SE direction and 50 km extension). While the major faults are Wadi El-Natrun bounding fault (N30° W direction with 120m for fault thrown), El-Alam fault (N45° E direction with 60 km in length and 35m in displacement) and the series of normal faults east Wadi El-Natrun. These faults accelerate the groundwater flow and cause the hydraulic connection between different adjacent water bearing formations.

Hydrogeological characteristics

The hydro-geologic cross-section in NW-SE directions (Fig. 2) shows that the study area includes two main successive water bearing formations, the Pleistocene alluvial sand and gravels in the east and

the Pliocene sand and clay Aquifer in Wadi El-Natrun (PAWN) in the west and northwest. The two water bearing formations are hydraulically connected and form an aerially extended aquifers that affected by local stratigraphic differences and geologic structures **(Diab *et al*., 2002, Ahmed, 1999;Ibrahim, 2005).** PAWN occupies the northwestern part of the area, where the depth increases from west to east and from south to north. It is composed of alternating layers of water bearing sandy horizons and water confining clay beds, so its groundwater exists under semi-confined condition. The recharge to this aquifer may be attributed to the excess irrigation water and the lateral flow from the Pleistocene aquifer with which it is hydraulically connected beside local rain storms. The discharging may result from a lateral flow towards Wadi El-Natrun depression, which acts as a natural discharging area of the Nile Delta aquifer or take place through the natural springs, open galleries, drilled wells, evaporation and evapotranspiration.

In addition, the hydraulic parameters of the PAWN, the transmissivity and the storativity, are essential for performing any numerical simulation. To estimate these parameters, four long duration pumping tests were carried out. Three in El-Ralat depression, DW18, DW19 and DW20, and the fourth is north El-Nasr Canal. The field data were analyzed according to (**Jacob, 1950 and Theis, 1935)** methods (Table 1).

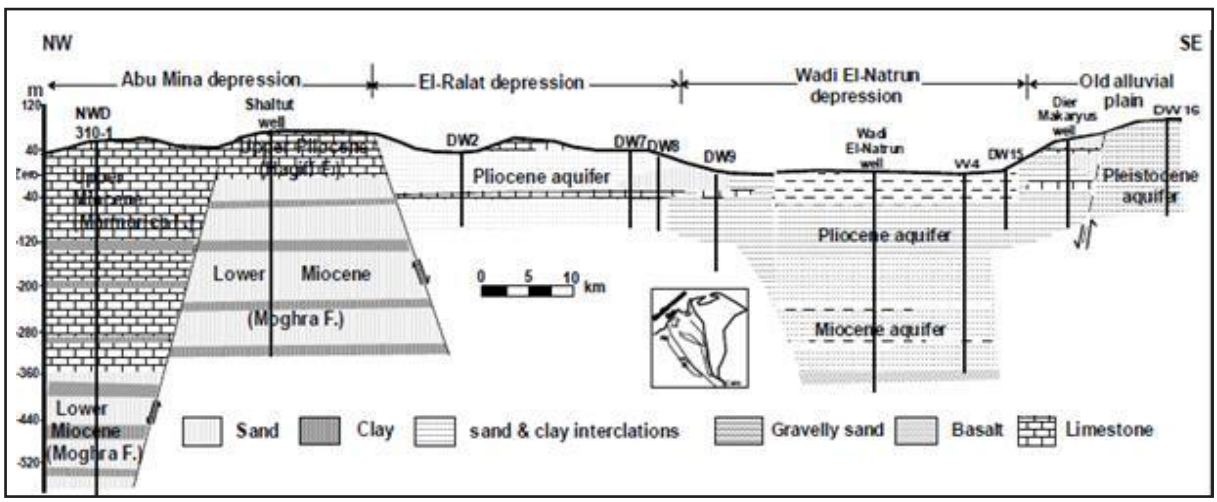

Fig. (2): Hydrogeological cross section showing different aquifers succession in the study area.

Table (1) *The results of long duration pumping test data of the study area.*

Well No.	ST (m)	K (m/d)	T (m^2/d)	S	T/S
DW3	75	9.9	741	$26x10^{-4}$	$28.5x10^{4}$
DW18	87	9.65	840	$1.9x10^{-4}$	$442x10^{4}$
Dw19	80	58.8	4705	$7.4x10^{-5}$	$636x10^{5}$
DW20	80	35.95	282	$1.3x10^{-6}$	$217x10^{5}$

ST=Saturated thickness (m), K= Hydraulic conductivity,
S =Storativity (--), T = Transmissivity (m^2/day).

Materials and methods

The materials used in this paper were collected through carrying out field trips in Wadi El-Natrun area during May 2015 to collect periodic groundwater samples. The hydraulic data of some of the groundwater wells' sites were obtained during this field trip **(Table 1).** In addition, the archival data, such as long term groundwater level records were collected from literature beside the recent records from team work of the Alexandria University. The basic hydrologic data of the studied wells were obtained during this field trip. For Hydrochemical measurements 58 groundwater samples include fifty two groundwater samples from Wadi El-Natrun, one brine sample from Lake El-Hammra, four brine samples from Lake El-Bida, one brine sample of Lake Rozetta were selected from the studied area. Electrical conductivity (EC), temperature and pH values were measured in the field using a portable conductivity and pH meters. In the laboratory, the water samples were filtered through 0.45 µm to separate suspended particles. Acidification (pH<2) with concentrated nitric acid was performed on the filtered samples for heavy metals analysis using ICP (Inductively Coupled Plasma) at the central laboratory of Desert Research Centre. The acid titration method was used to determine the concentration of bicarbonate HCO_3^- **(APHA, 1995).** Major anions (Cl^-, SO_4^{2-}) major cations (Ca, Mg, Na, K) and trace elements (Al, B, Ba, Fe, Mn, Mo, Ni, Pb, Sn, Sr, Ti, V and Zn) were analyzed using ion chromatography (Dionex DX-600). All reported values **(Table 2)** have an ionic balance within 5%. In addition, numerical modeling of pollutant migration in porous media has recently received a great deal of attention due to an increased interest in the preservation of the quality of the groundwater and the protection of it from various pollutants. Numerical models are able to account for the complexity of the subsurface and accommodate complicated boundary conditions. The finite difference methods have traditionally been applied to solve flow and transport equations. One of the most important implementations of the finite difference approach is in the powerful code visual MODFLOW ***(*McDonald and Harbaugh, 1988)** and its succeeding works. The methodological approach used in this paper is based on the mathematical modeling techniques applying this code. This model is capable of modeling time-dependent flow as well as mass transport problems. Eq.1 describes groundwater flow under non-equilibrium conditions in a heterogeneous and anisotropic medium and provided the principal axes of hydraulic conductivity are aligned with the coordinate directions **(Bear, 1979):**

$$\frac{\partial}{\partial x}\left(kxx\frac{\partial h}{\partial x}\right)+\frac{\partial}{\partial y}\left(kyy\frac{\partial h}{\partial y}\right)+\frac{\partial}{\partial z}\left(kzz\frac{\partial h}{\partial z}\right)-w=SS\frac{\partial h}{\partial t} \quad \ldots\ldots\ldots\ldots\ldots\ldots\ldots (1)$$

Where; K_{XX}, K_{yy} and K_{zz} are the hydraulic conductivity along the x, y, and z coordinate axes, (LT^{-1}); h is the potentiometric head (L); W is a volumetric flux per unit volume and represents sources and/or sinks of water (T^{-1}); S_s, is the specific storage of the porous material (L^{-1}); and t is time (T). In general, S_S, K_{XX}, K_{YY}, and K_{ZZ} may be functions of space and W may be a function of space and time. Moreover, to predict the environmental consequences of groundwater contamination one ought to know as to where the contaminant would interfere, when it would arrive; and what are the potential concentrations. The contaminant is introduced into groundwater by: (i) advection which is caused by flow of groundwater; (ii) dispersion, which is caused by mechanical mixing and molecular diffusion; and (iii) retardation which is caused by adsorption. The mathematical relationship between these processes can be written as follows **(Patil and Chore, 2014)**:

$$\frac{\partial}{\partial xi}\left[Dij\frac{\partial C}{\partial xi}\right]-\frac{\partial}{\partial xi}(Cvi)-\frac{CW}{n}=R\frac{\partial C}{\partial t} \quad \ldots\ldots\ldots\ldots\ldots\ldots (2)$$

$$Vi=\frac{-Kij}{n}\frac{\partial h}{\partial xi} \quad \ldots\ldots\ldots\ldots\ldots\ldots\ldots\ldots\ldots\ldots\ldots\ldots (3)$$

$$R=\left[1+\frac{\rho b\ Kd}{n}\right] \quad \ldots\ldots\ldots\ldots\ldots\ldots\ldots\ldots\ldots\ldots\ldots\ldots (4)$$

Where, C is contaminant transport, Vi is seepage or average pore water velocity in the direction xi, Dij is dispersion coefficient, Kij is hydraulic conductivity, C' is solute concentration in the source or sink fluid, W' is volume flow rate per unit volume of the source or sink, n is effective porosity, h is hydraulic head, R is retardation factor, and xi is Cartesian coordinate. For solving the transport problems having simplified boundary conditions and geometries, exact analytical solutions are available in the literature **(Bear, 1979).** While the historical response of the system could be inferred from the available field records, there is no way of computing the future behavior of the full-scale system unless it is actually subject to conditions. A full-scale experiment would be prohibitively costly and time consuming. The only feasible recourse, therefore is to construct a model, which reasonably portrays the behavior of full-scale system and simulate the relevant physical parameters, and describes the overall significant characteristics of the transport phenomena.

Construction of groundwater flow and contaminant transport model

The construction of the groundwater flow model of the PAWN requires the definition of the conceptual model, the model domain with flow boundary conditions and the aquifer material properties.

Conceptual model of PAWN

The conceptual model of the PAWN has been constructed. It based on the geology and the Petro physics of the Pliocene Formation. Its thickness is about 75 m in the northern portion, 150 m in some localities in Wadi El Natrun and gradually increases northwestward with a maximum thickness of about 300 m at El Qattara Depression **(Omara and Sanad, 1975).** The basaltic sheets are separating the overlying Pleistocene aquifer and the Daba'a shale Formation, it has variable thickness ranging between 20 to 30 meters and located at different vertical levels **(Fig.3).** The hydrogeologic system was concerned unconfined and confined of one layer type. The variations of the hydraulic conductivity are resulting from the variation in the saturated thickness through the flow section as well as the variation in the transmisivity resulting from the change in the Potentiometric level.

Model grid and boundary conditions

The simulation procedure was started by dividing the PAWN domain into a suitable grid pattern on which all the input items are performed via input menus. The total surface area of the model domain reaches 1800 km^2 (60 km in length and 30 km in width). The computational grid for the aquifer domain in the study area is divided into 1800 cells (60 columns and 30 rows). The dimension of the cell nodes reaches 1km for the cultivated and reclaimed areas **(Fig. 3).** The boundary conditions are represented by the outer boundaries which are chosen to be natural boundaries of the system taking into account that the boundaries should be taken remote enough from the effect of wells field. These constant head boundaries were assigned in the NE direction with constant value of 8 m asl, in the east direction with variable values ranged between 8 to 2 m asl, in the south western direction with variable values ranged between 16 to 20 m usl and finally in the south west direction with values ranged between 20 to 22 m asl **(Fig. 4).**

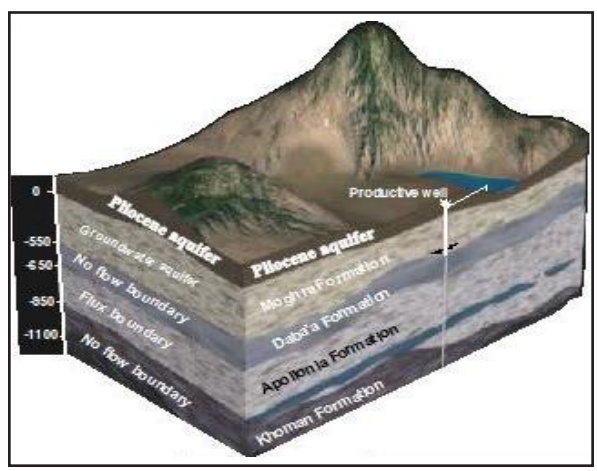

Fig. (3): Conceptual model of PAWN.

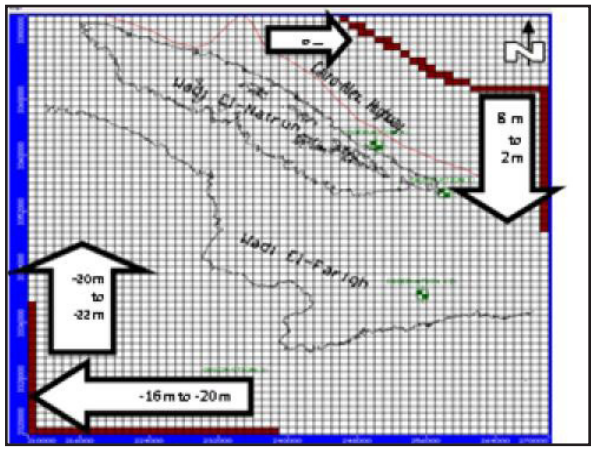

Fig. (4): Model grid with boundary conditions.

Aquifer characteristics

The input parameters for the PAWN simulation include aquifer hydraulic parameters (permeability and storage coefficients), aquifer geometry (vertical and areal extent of the aquifer) and aquifer stresses (recharge and discharge). The hydraulic parameters of the PAWN are given in Table1.The available digital elevation model (DEM) files data was used in WMS to automatically delineate topography and ground elevation of the model domain and the depth to impermeable bed (bottom of the aquifer) was used to estimate the aquifer thickness of every cell in the modeled area. The recharge to the modeled aquifer system may be from the Nile Delta area in the East and the Tahrir Province in the north as well as rainfall events. The discharge from the aquifer may be from natural discharge represented in the evapotranspiration from Wadi El-Natrun depression and it is neglected. Artificial discharge is mainly through water extraction for the development projects and this is the source of discharge in the model domain. The total annual losses due pumping reaches 304 Million m^3/year, from number of wells reached 696 wells **(Youssef *et al.*, 2012).**

The water level measurements through the bore hole piezometers in the model domain during November, 1991 were used to construct a contour map for the initial hydraulic head distribution **(Fig. 5- left map).**

Calibration and verification of the model

The initial data of the hydraulic parameters such as hydraulic conductivity (K) and specific yield (S) have been entered into the model with initial values based on data collected **(Table 1).** These data have very wide different ranges all over the modeled area. Every once these data entered into the constructed model, is allowed to run. If there is a convergence between the observed heads and calculated heads, an input data error is present which should be repaired time after time until the running process goes successfully. This means that the model successes for computing the heads of the aquifer at every cell. After many times of changing the K values, the variance between the observed and the calculated heads was minimized to 7.33% **(Fig. 5-right map).**

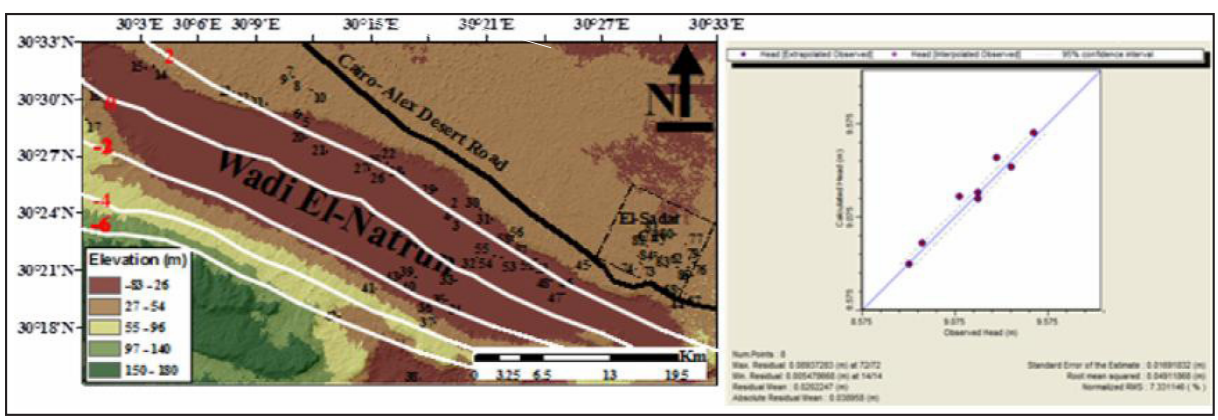

Fig. (5): Observed piezometric head contour map of PAWN (after Mostafa 1993) (left map) and calculated head vs observed head for the unsteady calibration (right map).

In addition, changing of the conductivity, dispersivity and adsorption coefficients were done for sensitivity analysis and to parameter adjustment applying MT3D code for contaminant transport simulation. This process allowed the groundwater model to be delineated for the maximum, minimum and most probable extent of the plume. The model was run for numerous iterations and outputs were recorded at different time intervals to show the size and extent of the heavy metal plume.

Testing scenarios

After completing the stage of calibration, the output of the first round was used to replace the initial condition with the condition of implementing the exploitation policies. The testing scenarios included four predicted groundwater regimes. The first predicted groundwater regime (base case scenario) was the initial proposed strategy of total pumping rate of 303703 m^3/day from 696 productive wells with an operating time of 10 hours and study the expected change in groundwater level during time of simulation (50 years) in arbitrary observation wells covering the model domain. The second proposed groundwater scenarios tested the predicted recharge from flash flood event during August 2015 (30 mm/h) on the groundwater regime of PAWN. The third scenario predicts the effect of recharge during the next 50 years while the Fourth proposed scenario tested the environmental impact of pollutants transport through PAWN.

RESULTS AND DISCUSSIONS

Complete chemical analysis of the selected groundwater samples, including pH, EC in situ, TDS, major cations and major anions were carried out using **(APHA, 1995)**. The results of PAWN groundwater and Lakes samples are presented in **Table (2).**

Table (2) *Chemical and saturation index results of the collected water samples.*

Well.	pH	EC	TDS	Cations (meq/l)				Anions (meq/l)			SI			
No		µs/cm	mg/l	Na^+	K^+	Ca^{2+}	Mg^{2+}	HCO_3^-	SO_4^{2-}	Cl^-	Calcite	Dolomite	Apatite	Quartz
1	7.4	1270	826	9.13	0.10	2.65	1.41	1.30	5.01	6.95	-0.412	-0.002		
2	6.9	7750	5014	54.35	0.33	17.78	7.13	1.65	38.48	39.62	-0.41	-0.121	**6.115**	**0.569**
3	8.8	1214	833	12.39	0.08	0.58	0.36	1.55	4.11	7.51	**0.345**	**1.584**	**9.124**	**0.326**
5	8.2	4540	2694	30.44	0.18	8.57	5.13	1.05	14.14	28.84	**0.652**	**2.184**	**11.867**	**0.405**
6	8.2	1570	872	10.87	0.08	2.21	1.31	2.00	3.38	9.04	**0.44**	**1.757**	**10.176**	**0.327**
7	7.9	8550	5154	58.70	0.26	15.26	9.57	1.35	26.93	56.99	**0.832**	**2.569**	**12.063**	**0.466**
8	7.4	5750	3026	37.39	0.23	7.89	4.99	1.30	10.40	38.92	-0.083	**0.745**	**8.48**	**0.454**
9	7.6	1068	597	8.26	0.08	1.09	0.66	2.10	1.09	7.09	-0.417	**0.052**	**6.434**	**0.365**
10	8	6800	4362	47.83	0.23	12.80	7.94	0.90	29.19	41.01	**0.464**	**1.821**	**10.393**	**0.432**
11	7.9	1420	825	11.30	0.10	1.42	0.81	1.70	2.64	9.17	-0.059	**0.745**	**8.09**	**0.39**
12	7.9	1377	809	11.30	0.10	1.37	0.87	1.80	1.66	10.01	-0.025	**0.816**	**7.53**	**0.4**
13	8.1	3620	1945	22.61	0.15	5.28	3.01	1.20	11.32	18.77	**0.528**	**1.909**	**10.74**	
14	7.9	3740	2008	25.22	0.23	4.53	3.05	1.40	5.66	27.11	**0.239**	**1.415**	**10.276**	**0.399**
15	7.2	2545	1405	19.57	0.15	2.02	1.63	2.20	5.62	15.29	-0.638	-0.268	**5.533**	**0.341**
16	7.4	3650	2331	32.18	0.23	3.45	2.86	1.95	7.28	29.89	-0.48	**0.064**	**7.788**	**0.292**
17	7	3880	2150	28.70	0.26	3.25	2.85	1.55	8.56	25.72	-0.901	-0.756	**5.212**	**0.35**
18	8.1	1240	687	9.35	0.08	1.14	0.70	1.60	2.81	6.81	-0.099	**0.69**	**8.334**	**0.352**
19	7.6	1795	973	12.61	0.13	1.74	1.09	1.50	5.20	9.17	-0.491	-0.088	**6.764**	**0.32**
20	8.3	1788	942	11.74	0.13	2.04	1.05	1.50	5.62	7.78	**0.256**	**1.317**	**9.883**	**0.334**

21	7.9	2680	1648	18.26	0.20	5.73	3.21	1.00	7.70	18.42	**0.07**	**0.989**	**9.026**	**0.313**
22	7	6990	4246	45.65	0.28	15.61	6.33	1.45	27.31	40.31	-0.408	**-0.107**	**8.381**	**0.515**
27	8.2	1174	652	8.70	0.13	1.50	1.15	2.10	1.25	7.37	**0.254**	**1.5**	**8.84**	**0.27**
28	7.3	5350	3183	32.18	0.10	13.10	7.37	1.25	15.14	36.84	-0.176	**0.505**	**8.467**	**0.376**
29	8.2	1411	803	10.22	0.10	2.19	1.10	1.40	3.59	8.06	-2.224	-3.649	**9.357**	**0.361**
30	7.30	5160	3074	27.83	0.2	13.7	7.11	1.1	20.86	28.84	-2.61	-4.423	**8.534**	**0.431**
31	7.6	6600	4060	39.13	1.28	16.79	7.05	0.90	26.00	39.62	-2.332	-3.941	**9.413**	**0.41**
32	7	5280	3288	32.61	1.38	14.98	4.49	2.00	16.23	36.14	-3.145	-5.771	**1.675**	**0.733**
33	7.4	4270	2576	27.83	1.33	6.94	6.96	1.70	8.67	33.36	-2.075	-3.04	**6.934**	**0.346**
34	7.9	6670	4068	42.61	1.38	12.42	8.78	1.40	21.76	44.48	-2.27	-3.585	**10.516**	**0.457**
35	7.8	7280	4343	50.00	1.40	10.47	9.63	0.90	19.09	52.13	-1.71	-2.347	**9.387**	**0.486**
36	7.8	789	455	4.78	0.15	1.17	2.09	2.10	0.87	4.87	-2.164	-2.974	**6.718**	**0.35**
37	7.8	1397	731	9.35	0.15	1.60	0.93	1.40	2.60	7.92	-2452	-4.04	**7.259**	**0.349**
38	7.2	1786	995	10.00	0.18	3.91	2.06	1.40	6.24	8.62	-2.488	-4.16	**5.286**	**0.418**
39	7.5	3740	2189	30.44	0.51	3.01	2.50	1.85	6.24	28.50	-2.316	-3.597	**6.551**	**0.335**
40	7.6	7290	4215	60.87	0.77	5.20	6.08	1.40	6.24	63.25	-0.214	**0.762**	**7.453**	**0.34**
41	7.9	801	384	4.70	0.13	1.02	0.70	1.15	1.05	3.82	-0.407	**0.119**	**6.659**	**0.339**
42	7.7	806	374	5.04	0.13	0.70	0.48	1.50	1.33	3.13	-0.655	-0.375	**5.737**	**0.341**
43	8.3	4130	2370	33.045	0.536	2.982	2.609	1.800	4.249	34.403	**0.417**	**1.89**	**9.249**	**0.39**
44	7.7	1310	741	6.305	0.179	3.988	2.017	1.200	4.680	6.116	-0.109	**0.583**	**7.531**	**0.41**
45	8.3	592	299	3.304	0.077	1.065	0.533	1.300	1.897	1.564	**0.045**	**0.883**	**8.146**	**0.423**

Continued.

Well.	**pH**	**EC**	**TDS**	**Cations (meq/l)**				**Anions (meq/l)**			**SI**			
No		**µs/cm**	**mg/l**	Na^+	K^+	Ca^{2+}	Mg^{2+}	HCO_3^-	$SO4^{2-}$	Cl^-	**Calcite**	**Dolomite**	**Apatite**	**Quartz**
46	7.9	1317	787	8.044	0.102	3.374	1.626	1.100	3.395	8.688	-0.013	**0.76**	**8.538**	**0.399**
48	7.3	4170	2692	26.088	0.281	10.225	5.059	1.200	22.256	19.808	-0.312	0.163	**6.238**	**0.4**
49	7.6	975	532	5.435	0.102	2.080	1.041	1.300	3.588	3.684	-0.413	-0.032	**6.476**	**0.367**
50	7.7	3700	2529	22.175	0.230	10.878	6.398	1.300	20.617	19.113	**0.15**	**1.162**	**9.894**	**0.357**
51	7.9	3700	2763	26.088	0.281	12.026	6.369	1.150	17.680	26.758	**0.33**	**1.489**	**11.801**	**0.307**
52	7	5400	3282	29.566	0.281	15.644	7.491	1.050	17.642	36.835	-0.488	-0.19	**7.351**	**0.503**
53	7.6	5140	3059	36.523	0.281	8.298	4.397	2.100	14.149	34.750	**0.097**	**1.016**	**12.802**	**0.494**
55	8	2050	1277	15.218	0.179	2.978	2.762	0.950	6.864	12.510	-0.11	**0.845**	**9.344**	**0.271**
56	7.7	1560	830	11.305	0.153	2.132	1.220	1.650	1.014	10.981	-0.204	**0.457**	**8.106**	**0.302**
57	7.7	2800	1635	18.262	0.153	6.068	2.775	1.100	6.032	20.155	-0.046	**0.672**	**8.69**	**0.352**
58	8.1	1050	590	7.826	0.153	1.247	0.736	1.250	1.456	6.881	-0.136	**0.604**	**8.545**	**0.297**
El-Hammra	9.6	125000	121800	1957	7.65	0.51	14.61	19.50	436	1473.40	**1.135**	**4.916**	**11.386**	**0.129**
El-Bida	7.8	8720	5525	69.57	0.38	11.15	6.29	1.20	35.33	52.13	**0.107**	**1.067**	**10.625**	**0.441**
El-Bida (600 m)	8.3	41600	25620	369.58	2.04	15.59	31.30	1.60	64.06	371.83	**0.583**	**2.611**	**12.342**	**0.352**
El-Bida (400 m)	8.4	43700	25722	373.93	2.04	14.05	30.49	1.10	62.40	375.30	**0.431**	**2.341**	**11.793**	**0.342**
El-Bida (200 m)	8.4	44200	26169	382.62	2.01	14.04	30.25	0.95	62.40	382.25	**0.344**	**2.166**	**12.497**	**0.346**
Rozetta	8.8	215000	339991	5457	7.650	22.95	119	13.997	374.4	5421	**1.59**	**4.969**	**12.852**	**0.986**

The groundwater of Pliocene aquifer in Wadi El-Natrun area, is characterized by the dominance of Na >Ca>Mg>K (86%), Na> Mg> Ca>K (7 %) and Na>Mg>K > Ca (7%) for cations and dominance of Cl>SO4>HCO3 (83%), Cl>HCO_3>SO_4 (12%), SO_4>Cl>HCO_3 (3%) and HCO_3> SO_4> Cl (2%) for anions. In general, pH values range between 6.9 and 8.8 with a mean value of 7.73 (slightly acidic to slightly alkaline), all samples fall within the recommended limit (6.5 to 8.5) for human consumption **(WHO, 2011)** except sample (no.3) was unsuitable for drinking purposes. EC values range from 429-8550 µS/cm at 25 °C, with a mean of 3339 µS/cm. EC values are above the permissible limits of **(WHO, 2011)** of 1,500 µS/cm in 65 % of groundwater samples. Total dissolved solids (TDS) values range from 214.6-5154 mg/l (classified as 10% only fresh water, 38% classed as slightly saline groundwater and about 52 % moderately saline groundwater according to **(Konikow and Reilly, 1999; Rhoades *et al*., 1992).**

Spatial distribution of TDS in mg/l as shown in Fig.6 illustrate that the Pliocene aquifer of Wadi El-Natrun in the southeastern part has low salinity in comparison with the northwestern parts.

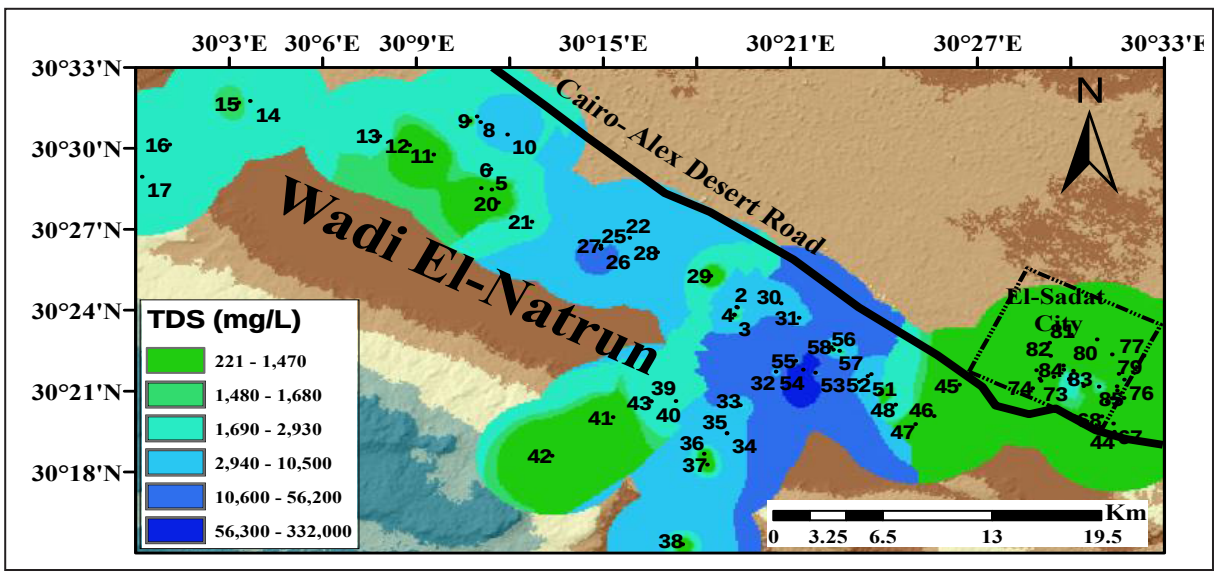

Fig. (6): Spatial distribution of TDS in (mg/l) in the study area.

This may be attributed to the influence of fresh water of Quaternary aquifer due east **(El Abd, 2005)** or the recharge from water of Miocene aquifer in the southeast of the depression. The dominance of slightly and moderately saline water at northwestern parts of the depression is due to the effect of the presence of great thickness of clay sediments of lagoonal and marine origin with high content of salt or due to facies change from fluvial deposits near the western border of Wadi El-Natrun into fluviomarine and shallow marine sands and sandy clay deposits towards Gebel El Hadid and Qattara depression due west **(Reda, 2007).** Wadi El-Natrun lakes are classified as alkaline water with PH value reaches to 9.6 at El-Hammra Lake and range between (7.8-8.4) At El-Bida Lake and 8.8 at Rozetta lake **Table (2).** For EC values Rozetta Lake shows the highest value reaches to 215000µs/cm compared with El-Hammra Lake 125000 µs/cm and El-Bida Lake (8720-44200 µs/cm) may be due to high evaporation rates in these lakes. Salinity is among the most important environmental factor and exerts various effects on the vitality of marine organisms. High values of TDS were recorded in Rozetta Lake (TDS= 339991 mg/l) than El-Hammra Lake (TDS= 121800 mg/l) and El-Bida Lake (5525-26169 mg/l). Generally, the very high

TDS values of Wadi El-Natrun lakes could be mainly attributed to the salty rock nature of this area or due to different evaporation rates during the different seasons. Therefore, water of these lakes is classified as hyper saline water (EC value is greater than 60000 µs/cm) according to **Bowman and Pschs (2008)**.

The Hydrochemical facies of groundwater can be evaluated by plotting the major cations and anions in (meq/l) on piper's trilinear diagram **Piper (1944)**. On Piper diagram, the plot **(Fig.7)** displays the effect of Wadi El-Natrun hyper saline Lakes on the surrounding groundwater chemistry that belongs essentially to the total dominance of (Cl^-, SO_4^{-2}) over (CO_3^{2-}, HCO_3^-) and alkalis (Na^+, K^+) over the alkali earth metals(Ca^{2+}, Mg^{2+}). These waters are generally Sodium-Chloride water type.

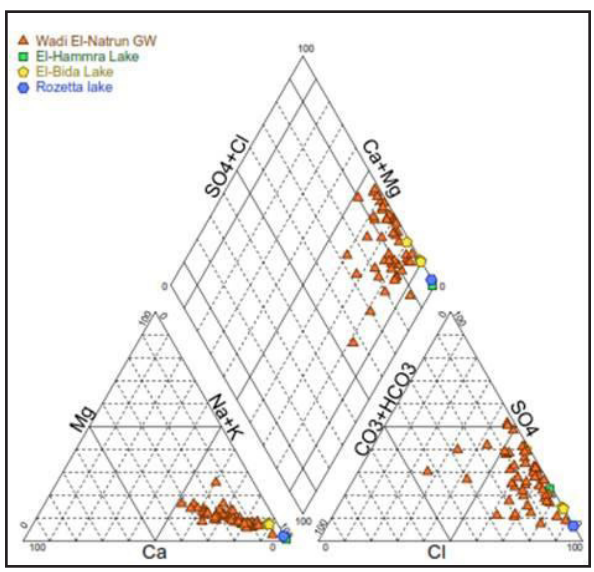

Fig. (7): Piper diagram showing chemical character of the collected water samples.

Gibbs (1970) constructed a diagram to show the Hydrochemical processes (water-rock interaction, precipitation and evaporation) affecting groundwater composition. Log TDS values were plotted against major cations (Na/ Na+Ca) and major anions (Cl/Cl+HCO_3) separately, Fig (8). The major ion chemistry together with Gibbs ratio plot indicate that, the groundwater chemistry in the area is mainly controlled by water-rock interaction beside evaporation from hyper saline lakes. Evaporation process might have incorporated some components of sodium and chlorine ions, also the evaporation increases salinity as a result of Na^+ and Cl^- and increases.

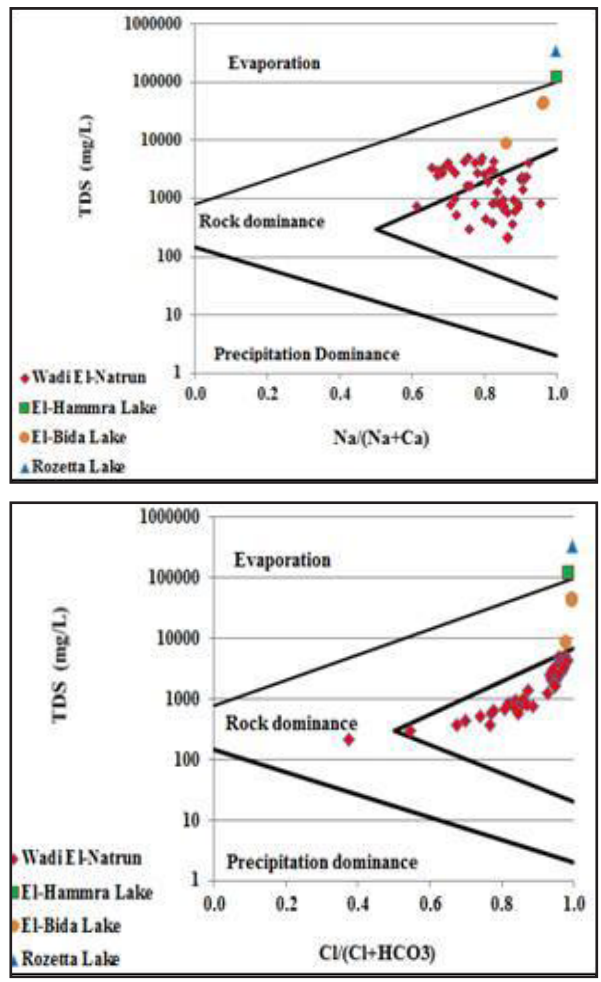

Fig. (8): Gibbs plot for cations (left side) and anions (right side) in the study area.

The processes of dissolution, precipitation and cation exchange actively take place in the groundwater system. The effect of water–rock interactions were investigated by calculating saturation indices (SI) for all Collected water samples using PHREEQC geochemical code **(Table 2).** These calculations provided saturation indices (SI) of minerals that might be reacting in the system.

The SI of a particular mineral can be defined as: SI= log (IAP/K_T) Where IAP is the ion activity product of the mineral water reaction and K_T is the thermodynamic equilibrium constant adjusted to the temperature of the given sample. It is postulated that mineral phases that are undersaturated (SI ≤ -0.1) will tend to dissolve and mineral phases that are supersaturated (SI ≥ 0.1) will precipitate these mineral phases out of solution. Equilibrium is taken to be between SI = -0.1 and 0.1. Results indicated that PAWN groundwater samples are supersaturated in Apatite $Ca_5(PO_4)_3OH$ and Quartz SiO_2. However, only 36%, 62% samples are supersaturated in calcite $CaCO_3$ and dolomite $CaMg(CO_3)_2$ respectively.

Trace Elements Distribution

The chemical inorganic pollutants of collected Wadi El-Natrun Lakes and groundwater samples are discussed through measurement of trace elements include: Al, B, Ba, Fe, Mn, Mo, Ni, Pb,Sn, Sr, Ti, V, and Zn with minimum, maximum and average values as shows in **(Table 3)** compared to national drinking water guidelines **Egyptian high committee of water (2007)** and international standards **(WHO, 2011)** to assess high concentrations of trace elements that could affect human health in the hypothetical case that impact shallow groundwater used for drinking water purposes. Concentrations of aluminum in lakes range from 0.08-0.329 mg/l with an average value of 0.21 mg/l **(Table 3).** In addition, groundwater samples concentrations between 0.056 and 0.206 mg/l were detected with an average value of 0.11 mg/l. Iron concentration values obtained from Wadi El-Natrun lakes range from 0.09-0.743 mg/l (average value of 0.3113 mg/l) and from 0.0163 to 1.95 mg/l (average value of 0.307 mg/l) in groundwater samples. These concentrations exceed WHO and Egyptian high committee of water limits of 0.3 mg/l in 19% of groundwater samples. High silica concentrations were detected in groundwater samples range from 12.22 to 26.24 mg/l (average value of 17.7 mg/l) while in Wadi El-Natrun lakes range from 12.3 to 19.2 mg/l (average of 15.7 mg/l). The relative increase in SiO_2 concentration may be related to an alkaline PH of water that accelerates the release of silicate from sediments to the overlying water. Strontium concentration value obtained from Wadi El-Natrun lakes range from 0.087-2.66 mg/l (average value of 1.78 mg/l) and from 0.092 to 3.77 mg/l (average value of 1.27 mg/l) in groundwater samples. It is important to note that the results of the chemical analysis of the groundwater samples show the presence of the same trace elements contamination (Table 3).

Table (3) *Trace elements concentrations in water samples (mg/l).*

Well no.	Al	B	Ba	Fe	Mn	Mo	Ni	Pb	Sn	Sr	Ti	V	Zn
1	<0.03	<0.03	0.0581	<0.02	0.0376	<0.003	<0.002	<0.006	<0.06	0.57	<0.004	<0.01	<0.0006
2	<0.03	1.477	0.029	<0.02	<0.003	0.0056	0.0038	0.0096	<0.06	3.40	0.0164	<0.01	<0.0006
3	<0.03	0.1229	0.039	<0.02	0.0214	<0.003	<0.002	<0.006	<0.06	0.13	<0.004	<0.01	<0.0006
5	<0.03	0.5406	0.0039	0.1	0.1198	<0.003	<0.002	<0.006	<0.06	1.75	0.0087	<0.01	<0.0006
6	0.0643	0.0819	0.0479	1.895	0.0357	<0.003	0.003	<0.006	<0.06	0.50	<0.004	<0.01	0.002
7	<0.03	0.9384	0.0629	0.0705	0.0249	<0.003	0.0039	<0.006	<0.06	3.12	0.0113	<0.01	0.0142
8	<0.03	0.624	0.0986	0.0773	<0.003	<0.003	<0.002	<0.006	<0.06	2.23	0.0083	<0.01	<0.0006
9	<0.03	<0.03	0.0264	0.0831	0.0223	<0.003	<0.002	<0.006	0.0989	0.24	<0.004	<0.01	<0.0006
10	<0.03	0.9195	0.0525	<0.02	<0.003	<0.003	0.0041	<0.006	<0.06	2.43	0.0121	<0.01	<0.0006
11	<0.03	0.0586	0.0662	0.03	<0.003	<0.003	<0.002	<0.006	0.0959	0.32	<0.004	<0.01	<0.0006
12	<0.03	0.0433	0.0457	<0.02	0.0118	<0.003	<0.002	<0.006	0.0851	0.34	<0.004	<0.01	0.0009
13	<0.03	0.7025	0.0346	0.2252	0.0491	<0.003	<0.002	<0.006	<0.06	1.19	0.0067	<0.01	0.0112
14	<0.03	0.2293	0.0409	0.6548	0.0709	<0.003	<0.002	<0.006	<0.06	1.16	<0.004	<0.01	<0.0006

15	<0.03	0.2535	0.0172	0.1582	0.0147	<0.003	<0.002	<0.006	<0.06	0.54	<0.004	<0.01	<0.0006
16	<0.03	0.5395	0.0214	0.346	0.0249	0.0046	<0.002	<0.006	0.0878	0.97	<0.004	<0.01	<0.0006
17	<0.03	0.3048	0.0182	1.951	0.3453	0.0209	0.0043	0.0104	<0.06	0.78	<0.004	<0.01	0.0035
18	<0.03	<0.03	0.0567	0.1013	0.0361	<0.003	<0.002	<0.006	<0.06	0.26	<0.004	<0.01	<0.0006
19	<0.03	0.0687	0.0709	0.0311	0.1075	<0.003	<0.002	<0.006	<0.06	0.39	<0.004	<0.01	<0.0006
20	<0.03	0.1643	0.0429	0.0755	0.1038	<0.003	<0.002	<0.006	<0.06	0.45	<0.004	<0.01	<0.0006
21	<0.03	0.207	0.0618	<0.02	0.0584	<0.003	<0.002	<0.006	<0.06	1.11	<0.004	<0.01	<0.0006
22	<0.03	1.105	0.0284	0.0305	<0.003	<0.003	0.0045	<0.006	<0.06	3.77	0.0166	<0.01	0.0608
27	<0.03	0.1585	0.0747	0.0247	0.0261	0.0042	<0.002	<0.006	<0.06	0.37	<0.004	<0.01	<0.0006
28	<0.03	0.467	0.0475	0.4356	0.2426	0.0045	0.0037	<0.006	<0.06	2.21	0.0089	<0.01	<0.0006
29	<0.03	<0.03	0.1121	0.0163	0.0352	<0.003	<0.002	0.0103	<0.06	0.46	<0.004	<0.01	0.0007
30	<0.03	0.5411	0.0467	0.3469	<0.003	<0.003	<0.002	<0.006	0.1543	2.44	0.0122	<0.01	0.0107
31	<0.03	0.3151	0.0373	<0.02	0.0193	<0.003	0.0049	<0.006	<0.06	3.46	0.0336	0.03	<0.0006
32	<0.03	0.6889	0.0264	0.0464	0.0106	<0.003	<0.002	<0.006	<0.06	2.99	0.0119	<0.01	<0.0006
33	<0.03	0.313	0.0973	0.0948	0.1665	<0.003	<0.002	<0.006	0.0738	1.69	<0.004	<0.01	0.0542
34	0.099	0.6798	0.0402	0.3773	0.0845	<0.003	0.0037	<0.006	<0.06	3.16	0.0104	<0.01	0.0017
35	0.0574	0.5154	0.0796	0.9038	0.255	0.0048	0.0034	<0.006	0.0826	3.24	0.0095	<0.01	0.0059
36	<0.03	0.1264	0.0338	0.2032	0.0574	<0.003	<0.002	<0.006	<0.06	0.83	<0.004	<0.01	<0.0006
37	<0.03	0.1046	0.0219	0.0368	0.006	<0.003	<0.002	<0.006	<0.06	0.35	<0.004	<0.01	0.0225
38	<0.03	<0.03	0.0336	0.1278	<0.003	<0.003	<0.002	<0.006	<0.06	0.83	<0.004	<0.01	<0.0006
39	<0.03	0.3468	0.0682	0.2492	0.0178	<0.003	<0.002	<0.006	0.0849	0.75	<0.004	<0.01	0.0007
40	<0.03	0.6638	0.0452	0.3018	0.0678	<0.003	0.0036	<0.006	<0.06	1.43	<0.004	<0.01	<0.0006
41	<0.03	<0.03	0.0105	0.2158	0.0052	0.0042	<0.002	<0.006	<0.06	0.25	<0.004	<0.01	0.0016
42	<0.03	0.7679	0.0398	0.2411	0.0286	<0.003	<0.002	<0.006	<0.06	0.85	<0.004	<0.01	<0.0006
43	<0.03	<0.03	0.0323	0.1132	0.0052	<0.003	<0.002	0.0075	<0.06	0.74	<0.004	<0.01	0.0806
44	<0.03	<0.03	0.0094	0.3055	0.0142	<0.003	<0.002	0.0076	<0.06	0.23	<0.004	<0.01	<0.0006
45	<0.03	<0.03	0.0683	0.0941	0.0247	<0.003	<0.002	<0.006	<0.06	0.68	<0.004	<0.01	0.0024
46	<0.03	<0.03	0.0221	0.1043	0.0381	<0.003	<0.002	0.0085	<0.06	0.09	<0.004	<0.01	0.0484

Continued.

Well no.	**Al**	**B**	**Ba**	**Fe**	**Mn**	**Mo**	**Ni**	**Pb**	**Sn**	**Sr**	**Ti**	**V**	**Zn**
47	<0.03	1.16	0.0146	0.0373	<0.003	0.0086	<0.002	0.0074	<0.06	2.18	0.0078	<0.01	0.0034
49	<0.03	<0.03	0.0551	0.0224	0.0114	0.0124	<0.002	<0.006	<0.06	0.31	<0.004	<0.01	<0.0006
50	<0.03	0.2367	0.0805	0.2781	0.0713	0.0108	<0.002	<0.006	<0.06	2.29	0.007	<0.01	0.0025
51	0.0568	0.2937	0.0541	0.1509	0.1117	0.0055	0.0048	0.007	<0.06	2.59	0.0161	<0.01	0.0463
52	<0.03	0.2742	0.0359	0.0213	<0.003	<0.003	0.0042	0.0092	<0.06	1.73	0.0104	<0.01	0..0089
53	0.2068	24.17	0.0091	0.5103	0.0193	0.011	<0.002	<0.006	<0.06	0.17	<0.004	<0.01	0.0058
55	<0.03	0.3468	0.0653	0.0997	0.1522	<0.003	0.0071	<0.006	<0.06	0.46	0.177	<0.01	0.1146
56	<0.03	0.3679	0.0382	0.5999	0.0202	<0.003	<0.002	<0.006	<0.06	1.34	<0.004	<0.01	0.0022
57	<0.03	0.1046	0.0219	0.0368	0.006	<0.003	<0.002	0.01	<0.06	0.35	<0.004	<0.01	0.0225
58	0.136	<0.03	0.0743	0.3118	0.0419	<0.003	<0.002	<0.006	<0.06	0.28	<0.004	<0.01	0.0154
El-Hammra	<0.03	53.88	<0.0005	<0.02	<0.003	0.0372	<0.002	<0.006	<0.06	0.087	<0.004	<0.01	<0.0006
El-Bida	0.2201	1.365	0.0355	0.2501	0.0365	0.0073	0.0045	0.0084	<0.06	2.639	0.0127	<0.01	0.0021

El-Bida (600 m)	0.3292	6.894	0.0289	0.2944	0.0915	0.0085	<0.002	<0.006	<0.06	2.628	0.0104	<0.01	0.0039
El-Bida (400 m)	0.0803	7.069	0.0272	0.1292	0.0842	0.0084	<0.002	<0.006	<0.06	2.646	0.0096	<0.01	0.001
El-Bida (200 m)	<0.03	7.18	0.0268	0.009	0.0802	0.0078	0.0036	<0.006	<0.06	2.66	0.0103	<0.01	<0.0006
Rozetta	<0.03	0.9888	0.0529	0.7437	0.245	<0.003	<0.002	0.0075	<0.06	0.873	<0.004	<0.01	0.0025
WHO (2011)	**0.2**	**-**	**0.003**	**0.4**	**-**	**-**	**0.01**	**-**	**> 0.1**	**0.11**	**-**	**-**	**-**
Egypt (2007)	**0.2**	**0.5**	**-**	**0.3**	**0.4**	**0.07**	**0.02**	**0.01**	**-**	**-**	**-**	**-**	**3**

Also, most spatial groundwater contaminants trend within the studied samples appear to be the result of receiving pollution from domestic sewage, septic tanks and fertilizers (Fig 9).

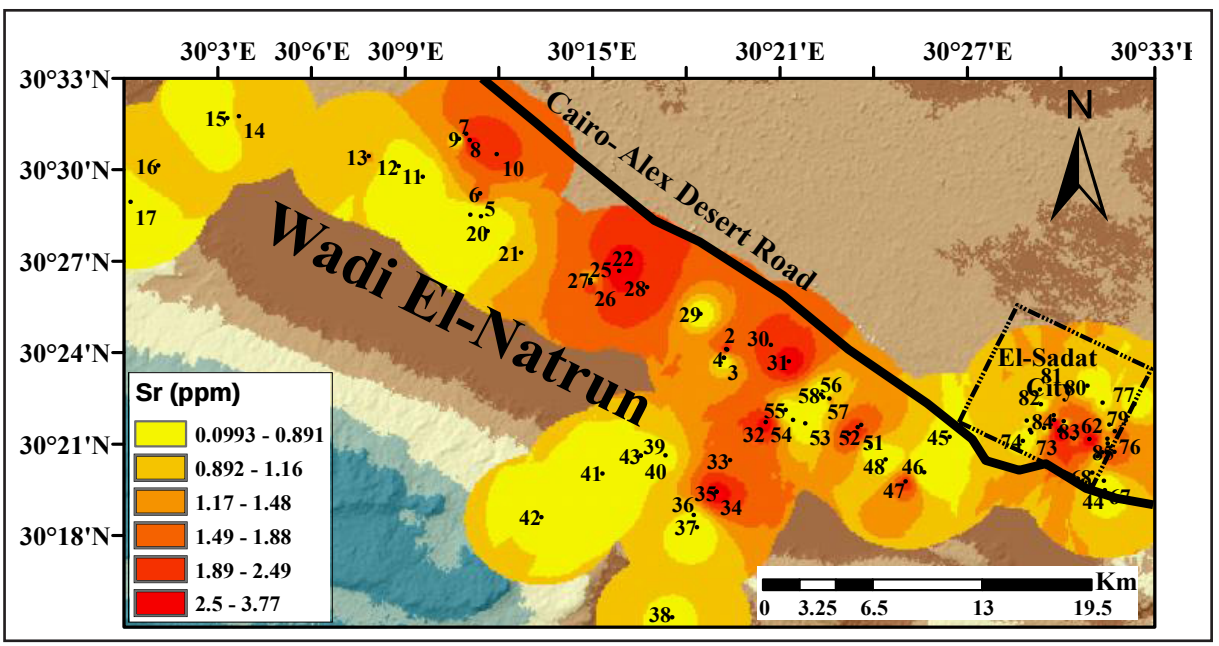

Fig. (9): Spatial distribution of Sr (mg/l) in groundwater samples of the study area.

It is concluded that the concentration of Al, Fe and Sr is higher that the acceptable limit according to WHO limits. So, the prediction of future concentration of these contaminants is required through applying numerical simulation of the contaminant transportation.

The diffusivity (T/S), which expresses the PAWN groundwater potentiality, ranges between 28.5×10^4 and 636×10^5 m^2/day (Northern part of Wadi El-Natrun and southern part respectively (see table 1). This indicates that the northern part of the PAWN has groundwater potentiality less than its value in the southern part. Accordingly, the location of the future reclamation activities in the northern part of PAWN may not be in the proper site. Moreover, the PAWN encompasses a large number of "flow domains" related to the appeared drawdown cone after simulation period of 50 years, as the pump rate increases to 349258 m^3/day (Fig. 6- left map). This condition will result in piezometeric head lowering within the area (3.04m after 50 years, **(Table 4)** followed by local groundwater flow from south, east and west directions towards the productive wells. The larger flow systems consist of relatively permeable depos-

its and constitute preferential zones for groundwater flow **(Gad *et al*., 2011).** The equi-potential contour lines show concentric shapes quite suddenly towards the northwestern part of the model domain **(Fig 10).** Higher hydraulic gradients due to the effect of flash flood event during 2015 (2nd scenario) in this location may be attributed either to a higher flow density or to a lower transmissivity of the PAWN system **(Gad and Abuel-Lohom, 2011).** Moreover, the appeared drawdown cone will continue to expand laterally for some period after stresses in case of applying third scenario. This means that water continues to be derived from storage in the PAWN. An abrupt decrease in the flow density is unlikely, because groundwater discharge is insignificant in the indicated transition zone (middle part of the model domain) and divergence of flow lines has a gradual and limited effect only in the north. The conclusion is that the southern part of the PAWN apparently is thicker and/or is composed of other, more permeable deposits than in the northern places **(Youssef *et al*., 2012).**

Table (4) *The predicted drawdown in PAWN after 50 years of simulation applying 1st scenario.*

Year	2025	2040	2065
Extra drawdown (m)	0.63	1.58	3.04

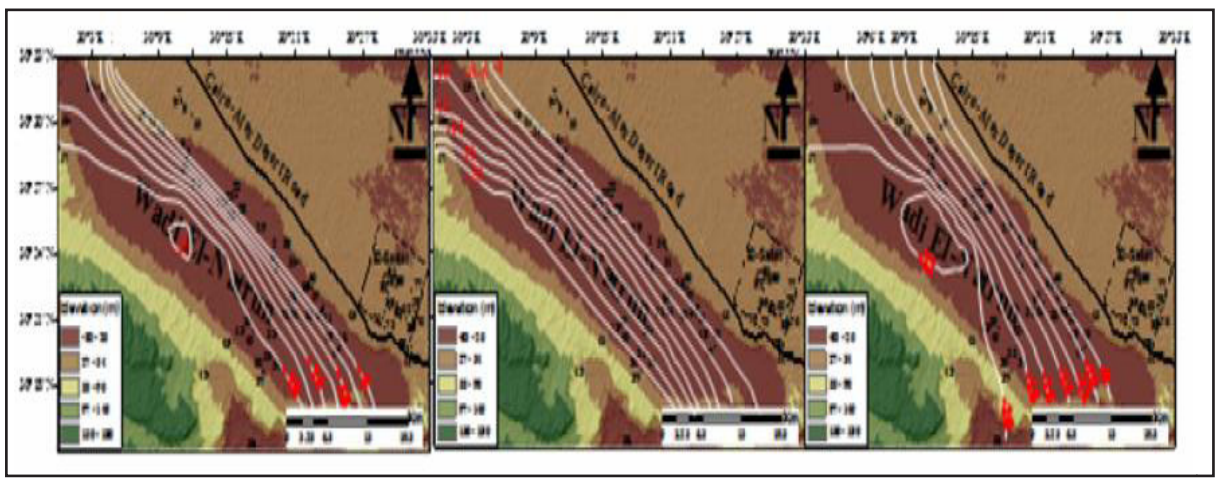

Fig. (10): Predicted piezometric head contour map of the PAWN based on 1st scenario (at 2015-left map), based on the 2nd scenario (middle map) and after 50 years from rainfall event (right map).

In addition, to predict the effect of flash flood event (30mm/h) on the piezometric head of PAWN, the result of the first scenario was used after changing the general head boundary condition in NW-SE direction from (-5 masl) to (-2 masl) to simulate the effect of rainfall and to calculate the new hydraulic head. The obtained hydraulic head values were shown in Table 5 and the head contour lines after rainfall event and after changing the general head boundary conditions in NW-SE direction are in (Fig. 11). The recharge to PAWN from the flash flood event at 2015 increases the piezometric head from 0.23m to 0.64m with mean value of 0.45m **(Table 5).**

Otherwise, the predicted piezometric head contour map of the PAWN applying 2nd scenario (Fig. 11-middle map) reflects the disappearance of the cone of depression related to 1st scenario which reappears again after 50 years (Fig. 11 – right map).

Table (5) *Values of observed and calculated heads before/after flash flood event at 2015.*

N	Obs.	Calc. before rainfall	Calc. after rainfall	After-before
1	-10.00	-10.32	-9.94	0.38
2	-11.00	-11.56	-11.31	0.25
3	-18.25	-18.21	-17.74	0.47
4	-12.50	-12.77	-12.38	0.39
5	-8.50	-8.28	-7.69	0.59
6	-18.00	-18.11	-17.57	0.54
7	-16.25	-16.33	-15.74	0.59
8	-6.50	-6.49	-5.86	0.63
9	-7.25	-6.96	-6.73	0.23
10	-17.75	-17.81	-17.36	0.45
11	-8.00	-7.40	-7.11	0.29
12	-6.75	-7.26	-6.85	0.41
13	-6.85	-6.83	-6.19	0.64

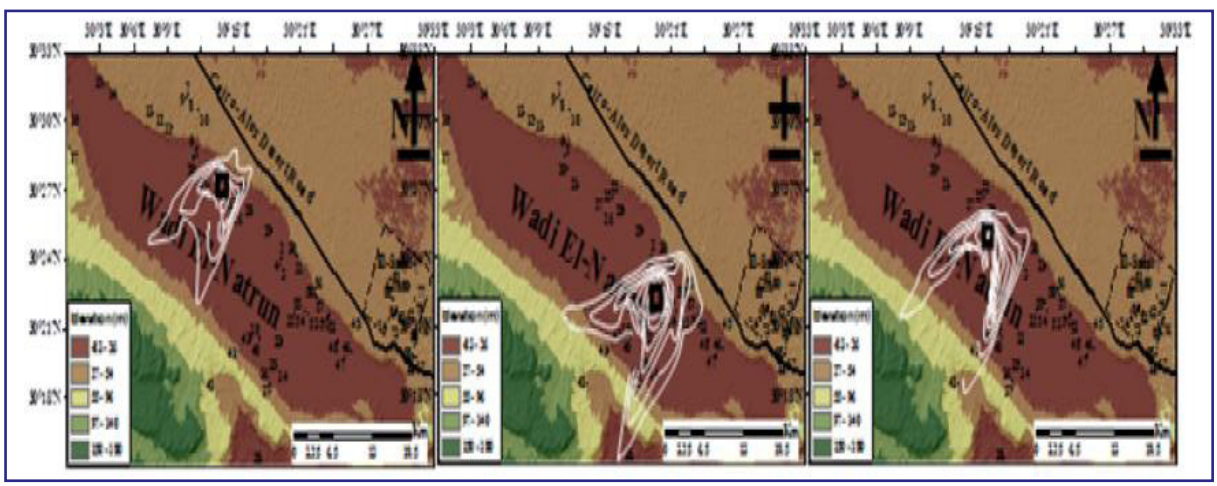

Fig. (11): Predicted plume expansion after 50 years for Al (left), Iron Fe (middle) and Sr (right).

In the other side, the results of the fourth scenario which deals with the simulation of the heavy metal contaminant transport are shown in **(Fig. 11).** It is obvious that the plume of the three contaminants (Aluminum, Iron, and Strontium) is different in shape and direction. These three contaminants cannot leach and move with groundwater in the short time because of high absorption capacity of the soil for adsorption there particles **(Khan and Ansari, 2005)** but mobility of them are assumed as the adsorption capacity of the soil is reached. It should be noted that the periods of contaminants migration prediction were selected after time period of 5, 10, 15, 20, 30, 40 and 50 years, **(Table 6).**

Moreover, to obtain the distinctive results and approving mobility of overloaded Aluminum, Iron and Strontium contaminants within the longer time in the study area, this enables the groundwater carried contaminants to bypass the soil particles which

permit transportation of high concentrations through the soil **(Knapp, 2002; Saghravani and Mustapha, 2011).** From **(Fig.11)** which represents the contaminants predicted movement in PAWN after 50 years of simulation, it is noticed that the contamination is migrating from the El-Hammra pond. The source plume appears to be a continuous source plume. The groundwater is moving towards southwest and west areas. The contaminations traveled at different distances as mentioned in **Table (6).** They travel 10.1, 11 and 12 km due west direction and 13.5, 9 and 10.2 km due SW direction after 50 years of simulation for Al, Fe and Sr contaminants respectively. This means that the contaminant only travels at a speed of about 0.11m/day. The affected areas by contamination are towards Monastery of St Bishoy area in the west, El Sourian Kloster area in the SW and their agricultural fringes. In addition, there are lateral flow starts after 20 year which threats a great part of the El-Diplomasseen agricultural lands.

Table (6) *The expected contaminants plume migration distance from the source point (El-Hammra pond) after time simulation of 5-50 years applying 4th scenario.*

Pollutant Name	Plume migration in west direction		Plume migration in SW direction	
	Time (year)	Distance (km)	Time (year)	Distance (km)
Aluminum (Al)	After 5 years	5.3	After 5 years	3.5
	After 10 years	6.8	After 10 years	5
	After 15 years	7.4	After 15 years	6.5
	After 20 years	8	After 20 years	9.6
	After 30 years	8.6	After 30 years	11.8
	After 40 years	9.3	After 40 years	12.8
	After 50 years	10.1	After 50 years	13.5
Iron (Fe)	After 5 years	6.5	After 5 years	5
	After 10 years	7	After 10 years	6.5
	After 15 years	7.5	After 15 years	7.3
	After 20 years	8.8	After 20 years	7.8
	After 30 years	9.4	After 30 years	8.2
	After 40 years	10.7	After 40 years	8.6
	After 50 years	11	After 50 years	9
Strontium Sr	After 5 years	8.3	After 5 years	6.5
	After 10 years	9.1	After 10 years	7.3
	After 15 years	9.9	After 15 years	8.2
	After 20 years	10.6	After 20 years	8.7
	After 30 years	11	After 30 years	9.3
	After 40 years	11.7	After 40 years	9.8
	After 50 years	12	After 50 years	10.2

CONCLUSION AND RECOMMENDATION

The sustainable development in PAWN suffers from some hydrologic problems especially groundwater depletion and pollution as a result of improper groundwater exploitation policies and pollution by heavy metals. Both over pumping and inadequate well locations are the main causes of this problem. A trial to mitigate this problem was carried out in this paper via predicting the change in groundwater levels and contaminants plume migration in the PAWN under different groundwater polices by combining groundwater chemistry with suitable groundwater flow model (MODFLOW). 52 groundwater and 6 surface water (Lakes) samples were collected to study hydrogeochemical processes affecting groundwater chemistry and contaminant indicators in Pliocene aquifer of Wadi El-Natrun. Groundwater chemistry in Pliocene aquifer is evolved into Na:Cl water type. This evolution is largely due to the effect of evaporation rate in saline lakes (El-Bida, El-Hammra and Rozetta) which lie in closed basins without outlet; the water in these lakes has a high salt concentration and is susceptible to the shallow aquifer in the depression. Trace element concentrations are exceeding the recommended levels of international standards for Al, Fe and Sr which may be attributed to intense agricultural activity. In addition, the depression receives pollution from domestic sewage, septic tanks and fertilizers. Four scenarios were tested to predict both the groundwater regime under stresses and contaminants plume migration. The first proposed scenario kept the proposed discharge from the present 696 productive wells (303703 m^3/day). The predicted groundwater level decline after simulation period of 50 years, applying this scenario, will reach 30m, 19m, 4m, 2m and 1m in the wells of the Wadi El-Natrun locality, wells of the middle locality, wells of the eastern locality, and wells of the southern locality respectively. The second proposed scenario kept the initial conditions and proposed an increase of the recharge component by flash flood event of 30 mm/h during the year 2015. The mean predicted increase in groundwater level reaches 0.45m. Moreover, the predicted contaminant plume migration reaches 10.1, 11 and 12 km due west direction and 13.5, 9 and 10.2 km due SW direction after 50 years of simulation for Al, Fe and Sr contaminants respectively.

To conserve the PAWN storage for longer time, it is recommended to reduce the number of the pumping wells (not more than 800 wells), reduce the initial and running time (not more than 12 hours), applying discrete irrigation system and achieving the objective of implementing the development policy with the groundwater recharge from the flash flood events. It is also highly recommended to construct a monitoring network to check the predicted contaminant plume migration distance to test the uncertainty of the model results.

REFERENCES

- **Ahmed, S. A. (1999):** Hydrological and isotope assessment of groundwater in Wadi El-Natrun and Sadat City, Egypt. Faculty of science, Ain Shams University, Cairo, Egypt,237.
- **APHA. (1995):** Standard methods for examination of water and wastewater, 19th edn. American Public Health Association, Washington, 2540C.
- **Bear, J. (1979):** Hydraulics of groundwater. McGrawHill, New York, N.Y., 569.
- **Bowman, J. and Pschs, J. (2008):** Chemical and physical properties of some saline lakes in Alberta and Saskatchewan.
- **Dassi, L. Zouari, K. Seiler, K.P. Faye, S. Kamel, S. (2005)**: Flow exchange
- between the deep and shallow groundwaters in the Sbeitla synclinal basin (Tunisia): an isotopic approach. *Environ. Geol* .47(4):501.
- **Dassi, L. (2010):** Use of chloride mass balance and tritium data for estimation of groundwater recharge and renewal rate in an unconfined aquifer from North Africa: a case study from Tunisia. *Environ. Earth.*

Sci. 60:861.

- **Diab, M. S. Gad, M.I. and El-Sheikh, A. E. A.(2002):** Study the Effect of New Reclamation Projects on the Groundwater System in the Area Northwest Wadi El Natrun and South El Nasr by Using Mathematical Modeling. In, edited by Diab. Faculty of Engineering, Mansoura University, El Mansoura, Egypt.
- **Edmunds, W.M. (2009):** Geochemistry's vital contribution to solving water resource problems. *Appl. Geochem.* 24(6):1058.
- **Egyptian Higher Committee for Water (EHCW) (2007):** Egyptian Standard for Drinking Water and Domestic Uses (in Arabic).
- **El Abd, E. A.(2005):** Geological impact on the water bearing formations in the area southwest Nile Delta, Egypt. Ph.D. Thesis, Fac.Sci., El Minufiya University., Sheibin El Kom, Egypt, 254.
- **El-Fayoumi, I. F. (1964):** Geology of Groundwater Studies in Wadi El-Natrun Area. Cairo, Egypt: Faculty of Science, University of Cairo.
- **Fehdi, C.h.; Rouabhia, A.; Baali ,F. and Boudoukha, A. (2009):** The Hydrogeochemical characterization of Morsott-El Aouinet aquifer, Northeastern Algeria. *Environ. Geol.* 58:1611.
- **Foster, S. and Chilton, P. J. (2003):** Groundwater: the Processes and Global Significance of Aquifer Degradation. *Philosophical Transactions of the Royal Society B: Biological. Sciences* 358 (1440) (December 29): 1957.
- **GAD, M. I. and Abuel-Lohom, N. (2011):** Water Resources Management in an Arid Area: Estimation of Groundwater Depletion in Sana'a Basin, Yemen. 1st Int., Renewable Energy & Technology Conf., (IRETC 1), Hurghada, Egypt.
- **GAD, M. I.; El Sheikh, A. E. and El Osta, M. M. (2011):** Optimal management for groundwater of Nubian aquifer in El Dakhla depression, Western Desert, Egypt. *IJWFEE*. 3(8), 111.
- **Gibbs, R.J. (1970):** Mechanisms controlling world water chemistry. *Science* 17:1088.
- **Ibrahim, S. (2005):** Groundwater Resources Management in Wadi El-Farigh Area and Its Vicinities for Sustainable Agricultural Development. Cairo, Egypt: Faculty of Engineering, Ain Shams University.
- **Jacob, C.E.(1950):** Flow of ground water, in Rouse, H., ed., Engineering Hydraulics, John Wiley, 321.
- **Jianhua, S. Qi, F. Xiaohu, W. Yonghong, S. Haiyang, X. Zongqiang, C.**
- **(2008):** Major ion chemistry of groundwater in the extreme arid region northwest China. *Environ. Geol.* 57:1079.
- **Khan, F.A. and Ansari, A.A. (2005):** Eutrophication: an ecological vision. *The Bot. Rev.* 71 (4): 449.
- **Knapp, B.J. (2002):** Nitrogen and Phosphrous; Grolier Educational, ISBN-10:0717275833; ISBN-13: 978-0717275830.
- **Konikow, L. and Reilly, T. (1999):** Seawater Intrusion in the United States. Seawater intrusion in coastal Aquifers-Concepts, methods and practices. Springer, 463.
- **Liu, C. Yu, J. Kendy, E. (2001)**: Groundwater exploitation and its impact on
- the environment in the North China Plain. *Water. Int* .26(2):265.
- **McDonald, M. G. and Harbaugh, A. W.(1988):** MODFLOW, A modular three dimensional finite difference groundwater flow model. U.S. Geolog.Survey, Open-file report, 83.
- **Mostafa, N. E. (1993):** Hydrogeological and hydrostudies on Wadi El-Farigh area, Western Desert, Egypt. M. Sc. Thesis, Faculty of Science, El-Minoufiya University, Shibin El-Kom, Egypt,132.
- **Omara, S. M. and Sanad, S. (1975):** Rock Stratigraphy and structural features of the area between Wadi El-Natrun and the Moghra Depression, Western Desert, *Egypt. Geol. J. B.* 16: 45.
- **Patil, S.B. and Chore, H.S. (2014):** Contaminant transport through porous media: An overview of experimental and numerical studies, *Adv. Environ. Res.,*

Int. J. 2(1): 45.

- **Piper, A.M.(1944):** A graphic procedure in the geochemical interpretation of water analysis. Amer. Geophys. Union Trans, 25: 914.
- **Reda, M.A.(2007):** Hydrogeochemical study for groundwater for the west-northern area of Wadi El-Natron –Western desert, Egypt. M.Sc. Thesis, Faculty of Science, Minufia University,Egypt.
- **Rhoades, J.D. Kandiah, A. and Mashali, A. (1992):** The Use of Saline Waters for Crop Production, FAO.
- **RIGW. (2004):** Groundwater inventory in Western Nile Delta. Internal report. Research Institute for Groundwater, El Kanter El Khairia, Egypt.
- **Saghravani ,S.R. and Mustapha, S. (2011):** Prediction of contamination migration in an unconfined aquifer with Visual MODFLOW: A case study. World. *Appl.Sci.J.* 14 (7): 1102.
- **Said, R. (1962):** The Geology of Egypt. El-Sevier Pub. Co., Amesterdam, New York.
- **Theis, C.V.(1935):** The relation between the lowering of the piezometric surface and the rate and duration of discharge of a well using groundwater storage, Am. Geophys. Union Trans, 16:519.
- **World Health Organization (WHO). (2011):** Guidelines for drinking water quality, World Health Organization Geneva, 4th Ed., Recommendations, 1-4.
- **Youssef, T.; GAD, M.I. and Ali, M.M. (2012):** Assessment of groundwater resources management in Wadi El-Farigh area using MODFLOW. IOSR J Eng (IOSRJEN) 2(10):69.
- **Zagonari, F. (2010):** Sustainable, just, equal and optimal groundwater management strategies to cope with climate change: insights from Brazil. Water Resour Manage 24:3731.

مجلة
التقنيات النووية
فى العلوم التطبيقية
مجلد 5 ، عدد 4 ، ص 183 : 203 ، (2017)

المحاكاة العددية لسريان المياه الجوفية وانتقال المذيبات في الخزان السطحي لوادي النطرون - غرب الدلتا، مصر

محمد إبراهيم جاد[1]، رشا عبدالله حسين[2] ، عبدالحميد مصطفى الأعصر[3]

إن منطقة الدراسة الواقعة بين طريق مصر-الاسكندرية الصحراوي وغرب وادي النطرون تتعرض لسباق محموم من المستثمرين لاستصلاح مناطق جديدة لقربها من الطرق السريعة وسهولة الوصول إليها. إلا أن إمكانيات الخزان الجوفي السطحي بها لا تتناسب مع حركة الاستصلاح المتزايدة مما يترتب عليه استنزاف الخزان الجوفي السطحي الموجود كمياً ونوعياً. وفي محاولة لدراسة تأثير إنتقال المذيبات على نظام المياه الجوفية بالمنطقة المذكورة باستخدام النمذجة الرياضية أمكن في هذا البحث إلقاء الضوء على التنبؤ بما سيحدث لنظام المياه الجوفية عند ازدياد معدلات السحبل وتراكيز العناصر الثقيلة ببحيرات وادي النطرون وذلك باستخدام النموذج الرياضي Visual MODFLOW وكانت النتائج كالآتي :

١. ظهور عدد كبير من "مجالات التدفق" المتعلقة بمخروط الإنخفاض بعد فترة محاكاة لمدة ٥٠ عاما، حيث يزداد معدل الضخ إلى ٣٤٩٢٥٨ متر مكعب في اليوم ، وسوف يؤدي هذا الشرط إلى خفض الضغط البيزوميتري داخل المنطقة (٣٫٠٤م) بعد ٥٠ عاما يليه تدفق المياه الجوفية المحلية من الجنوب والشرق والغرب نحو الآبار المنتجة.

٢. تظهر خطوط الكنتور المحتملة أشكال متحدة المركز فجأة نحو الجزء الشمالي الغربي من مجال النموذج ويعزى ارتفاع التدرجات الهيدروليكية كنتيجة لتأثير حدوث فيضان عام ٢٠١٥(السيناريو الثاني).

٣. علاوة على ذلك، فإن مخروط الإنخفاض سوف يستمر في التوسع أفقيا في حالة تطبيق السيناريو الثالث. وهذا يعني أن المياه لا تزال مستمدة من المخزون. ومن غير المرجح حدوث انخفاض مفاجئ في كثافة التدفق، لأن تصريف المياه الجوفية لا يذكر في منطقة الجزء الأوسط من نطاق النموذج، كما أن تباين خطوط التدفق له تأثير تدريجي ومحدود فقط في الشمال.

٤. تظهر نتائج السيناريو الرابع الذي يتناول محاكاة نقل ملوثات المعادن الثقيلة أن مسافة إنتقال سحابة الملوثات الثلاثة (الألومنيوم والحديد والإسترانشيوم) تختلف في الشكل والاتجاه ، ولا يمكن لهذه الملوثات الثلاثة أن تترشح وتتحرك بالماء الجوفى فى وقت قصير بسبب قدرة إمتصاص عالية للتربة للإمتزاز. وعلاوة على ذلك، فإن هجرة سحابة الملوثات المتوقعة بعد ٥٠ عاما من المحاكاة تصل إلى ١٠٫١ و ١١ و ١٢ كم في إتجاه الغرب و ١٣٫٥ و ٩ و ١٠٫٢ كم في إتجاه الجنوب الغربي على الترتيب .

وعليه تم التوصية بعدم التوسع في مشاريع الاستصلاح بالمنطقة بحيث لا تتعدى الاحتياجات المائية الفعلية لها كمية التغذية المحسوبة لخزان البليوسين (أي ما يعادل الاحتياجات المائية لحوالي١٠٠٠٠ فدان) وتقليل عدد آبار الضخ (لا يزيد عن ٢٣٠ بئر) والحد من زمن الضخ بحيث لا يزيد عن ١٠ ساعة، وتطبيق نظام الري المنفصل. أو الاعتماد على المصادر السطحية بجانب المياه الجوفية في حالة ازدياد المساحة التي ستستصلح عن المساحة المذكورة بإعادة تغذية المياه الجوفية من أحداث الفيضانات. كما يوصى أيضا بإنشاء شبكة آبار مراقبة للتحقق من مسافة هجرة سحابة الملوثات المتوقعة لاختبار عدم اليقين من نتائج النموذج والحد من زيادة تركيز الملوثات بالمنطقة.

1. قسم الهيدرولوجيا – مركز بحوث الصحراء- المطرية-القاهرة.
2. قسم المواقع و البيئة هيئة – الرقابة النووية و الاشعاعية – القاهرة .
3. قسم الهيدروجيوكيمياء – مركز بحوث الصحراء- المطرية- القاهرة.